Glass formation and magnetic properties of Fe-based metallic glasses fabricated by low-purity industrial materials

Man ZHU, Yang FA, Zeng-yun JIAN, Li-juan YAO, Chang-qing JIN, Jun-feng XU, Rui-hua NAN, Fang-e CHANG

School of Materials and Chemical Engineering, Xi'an Technological University, Xi'an 710021, China

Abstract: Fe-based metallic glasses of $(Fe_{74}Nb_6B_{20})_{100-x}Cr_x$ (x=1, 3, 5) with high glass forming ability (GFA) and good magnetic properties were prepared using low-purity raw materials. Increasing Cr content does not significantly change glass transition temperature and onset crystallization temperature, while it enhances liquidus temperature. The addition of Cr improves the GFA of the $(Fe_{74}Nb_6B_{20})_{100-x}Cr_x$ glassy alloys compared to that in Cr-free Fe−Nb−B alloys, in which the supercooled liquid region (ΔT_x), T_{rg} and γ are found to be 50−54 K, 0.526−0.538, and 0.367−0.371, respectively. The $(Fe_{74}Nb_6B_{20})_{100-x}Cr_x$ glassy alloys exhibit excellent soft magnetic properties with high saturation magnetization of 139−161 A·m²/kg and low coercivity of 30.24−58.9 A/m. Present Fe−Nb−B−Cr glassy alloys exhibiting high GFA as well as excellent magnetic properties and low manufacturing cost make them suitable for magnetic components for engineering application.

Key words: Fe-based metallic glasses; Cr; glass forming ability; magnetic property

1 Introduction

Fe-based metallic glasses are commercially the most important metallic materials due to their plentiful natural resources and other unique physical and mechanical properties [1−5]. Nowadays, they were served in the field of functional materials, such as magnetic core, electrical devices, switch transformer, and electronic micro- components. In order to extend their industrial applications, great endeavor has been devoted to the development of new Fe-based metallic glasses with high glass forming ability, good magnetic properties and low manufacturing cost.

In 1988, YOSHIZAWA et al [6] developed the soft magnetic material in the Fe−M−B (M=Zr, Hf, or Nb) alloy system with high saturation magnetization. Later, the glass formation, the structure upon crystallization, and the magnetic properties of the metallic glasses or nanocrystalline in ternary Fe−Nb−B alloy system [7−10] were intensively investigated. STOICA et al [11] reported ternary $Fe_{66}Nb_4B_{30}$ bulk metallic glasses (BMG) with a supercooled liquid region of 31 K, mechanical strength of 4 GPa, and Curie temperature of 646 K. YAO

et al [12,13] pointed out that the best glass former was pinpointed at $Fe_{71}Nb_6B_{23}$ with a critical diameter of 1.5 mm, which exhibits ultrahigh fracture strength reaching 4.85 GPa and compressive plastic strain up to 1.6%. However, most Fe-based metallic glasses are still expensive by using high-purity raw materials and are inefficient to produce, which limits their commercial applications. Due to relatively low glass forming ability, practical applications of conventional Fe-based metallic glasses have been limited in the form of rapidly solidified ribbons or thin film. In order to reduce production costs, some researchers attempted to fabricate Fe-based metallic glasses using industrial raw materials [14,15]. These Fe-based metallic glasses not only possess large GFA, high thermal stability and other desirable properties, but also have the advantage of low cost. Recent studies indicated that minor addition of the alloying element has shown beneficial effect on GFA and mechanical properties [13,16−19]. The addition of chromium (Cr) has been reported to significantly improve the soft magnetic properties and corrosion resistance [20−22], and large amount of Cr decreases the GFA. In the present study, with the aim of searching new Fe-based metallic glasses, we developed quaternary

$(Fe_{74}Nb_6B_{20})_{100-x}Cr_x$ (x=1, 3, 5) glassy alloys by using low-purity raw materials. The effects of Cr content on the GFA and magnetic properties were investigated to provide guidance for practical application of the Fe-based metallic glasses.

2 Experimental

Master alloy ingots with nominal composition of $(Fe_{74}Nb_6B_{20})_{100-x}Cr_x$ (x=1, 3, 5) were arc-melted six times under the Ti-gettered argon atmosphere by using pure Fe (99.8%), Nb (99.8%), Cr (99.8%), and Fe−17.5%B master alloy (mass fraction). The master alloy ingots were firstly purified with B_2O_3 by fluxing method in order to remove the impurities as much as possible, and then the melt-spun ribbons were prepared by injecting the molten alloys contained in a quartz tube on the surface of a single copper roller with a linear velocity of 40 m/s and ejection pressure of 20 kPa under the Ar protective atmosphere. The resulting ribbons with a thickness of 20−30 μm were obtained.

Phase constitution was identified by X-ray diffractometer (XRD, Bruker D8 advance) with Cu K_α as a radiation. Thermal behaviors of the glassy ribbons were studied using a differential scanning calorimetry (DSC, Mettler-Toledo TGA/DSC1) at a continuous heating rate of 40 K/min. Room temperature magnetic hysteresis loops were measured using a vibrating sample magnetometer (VSM, Lake Shore 7410) at a magnetic field of 7.96×10^5 A/m.

3 Results and discussion

3.1 Structure analysis

Figure 1 shows the XRD patterns taken from the melt-spun $(Fe_{74}Nb_6B_{20})_{100-x}Cr_x$ (x=1, 3, 5) alloys. It can be found that only a broad diffraction halo in the 2θ range of 35°−55° for the alloys with different Cr contents
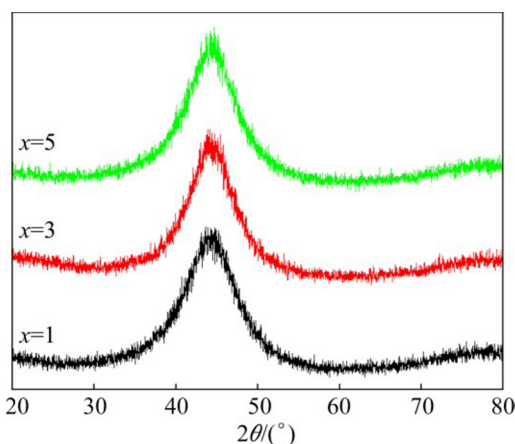

Fig. 1 XRD patterns of melt-spun $(Fe_{74}Nb_6B_{20})_{100-x}Cr_x$ (x=1, 3, 5) alloys

was detected and no other sharp diffraction peaks corresponding to a crystalline phase were found. The XRD results indicated that fully amorphous structure can be obtained for all the compositions with different Cr contents.

3.2 Effect of Cr addition on glass forming ability

Figure 2 illustrates the DSC traces taken from the $(Fe_{74}Nb_6B_{20})_{100-x}Cr_x$ (x=1, 3, 5) glassy alloys at a constant heating rate of 40 K/min. A distinct glass transition followed by the appearance of a supercooled liquid region and then crystallization events are clearly observed, as shown in Fig. 2(a). The glass transition temperature T_g, onset crystallization temperatures T_{x1} and T_{x2}, melting temperature T_m, and liquidus temperature T_l were listed in Table 1. All DSC traces reveal two exothermic peaks, indicating that they undergo a two-stage crystallization event. When the Cr content is equal to 1% (mole fraction), the values of T_g and T_{x1} are 824 K and 875 K, respectively. As is evident from this figure, increasing Cr content does not change remarkably the values of T_g and T_x, which is in accordance with that reported by LONG et al [22]. The supercooled liquid
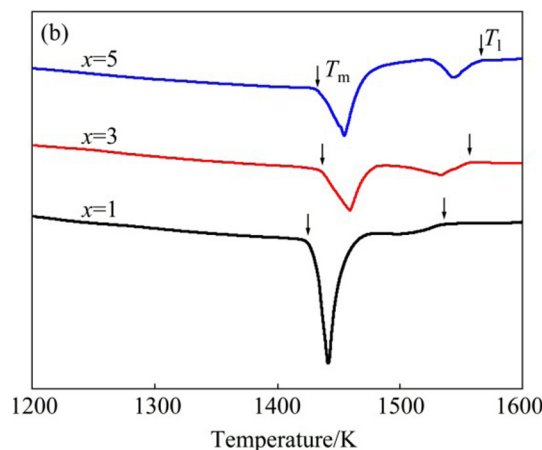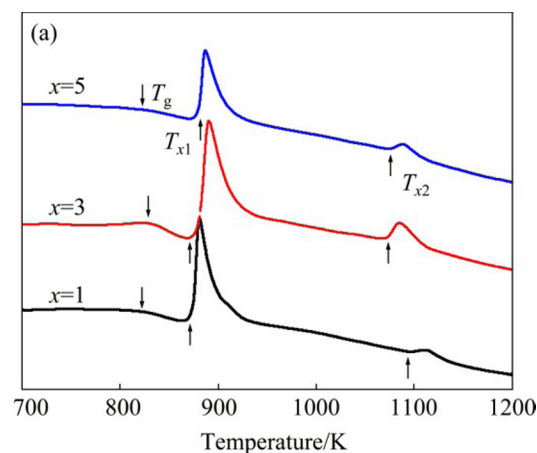
Fig. 2 DSC traces of $(Fe_{74}Nb_6B_{20})_{100-x}Cr_x$ (x=1, 3, 5) glassy alloys at constant heating rate of 40 K/min: (a) Low temperature region; (b) High temperature region

Table 1 Thermal properties for $(Fe_{74}Nb_6B_{20})_{100-x}Cr_x$ (x=1, 3, 5) glassy alloys

Material	T_g/K	T_{x1}/K	T_{x2}/K	T_m/K	T_l/K	ΔT_x/K	T_{rg}	γ
$(Fe_{74}Nb_6B_{20})_{99}Cr_1$	824	875	1093	1417	1533	51	0.538	0.371
$(Fe_{74}Nb_6B_{20})_{97}Cr_3$	827	877	1072	1427	1557	50	0.531	0.367
$(Fe_{74}Nb_6B_{20})_{95}Cr_5$	825	879	1074	1431	1566	54	0.526	0.368

region ΔT_x ($=T_{x1}-T_g$) ranges from 50 K to 54 K, which is larger than that in Cr-free $Fe_{74}Nb_6B_{20}$ alloys (i.e., ΔT_x= 24 K) reported by SONG et al [17]. The results suggest that adding an appropriate amount of Cr remarkably enhances the GFA. Figure 2(b) depicts the melting behavior of alloys with different Cr contents. Two endothermic events can be clearly observed for all compositions, suggesting that the three glass-forming alloys are all off-eutectic. As the Cr content increases from 1% to 5%, the values of T_m and T_l increase from 1417 to 1431 K and from 1533 to 1566 K, respectively. Other GFA parameters, T_{rg} [23] and γ [24], were calculated using characteristic temperature and were also listed in Table 1. Values of T_{rg} and γ are found to decrease from 0.538 to 0.526 and from 0.371 to 0.367, respectively, with increasing Cr content. The variation of ΔT_x with Cr content is different from that of parameters T_{rg} and γ with Cr content. From thermal parameter ΔT_x, it can be suggested that the $(Fe_{74}Nb_6B_{20})_{95}Cr_5$ alloy exhibits the best GFA.

3.3 Enhancement of GFA by Cr addition

In present study, thermal stability and glass forming ability were improved when a small amount of Cr was introduced into the $Fe_{74}Nb_6B_{20}$ alloys. The stabilization of the supercooled liquid phase can be achieved by increasing the atomic packing density and forming the short-range arrangement order in the liquid phase [17]. In order to explain the thermal stability and GFA in the multi-component alloys, three parameters including atomic size difference (δ), the mixing enthalpy (ΔH_{mix}), and the mixing entropy (ΔS_{mix}) [25], were used to characterize the collective behavior of the constitute elements. These parameters were defined by Eqs. (1−3), respectively.

$$\delta = 100\sqrt{\sum_{i=1}^{n} c_i (1 - r_i / r)^2} \tag{1}$$

where $r = \sum_{i=1}^{n} c_i r_i$ represents average atomic radius, c_i and r_i are the atomic fraction and atomic radius of the i-th element.

$$\Delta H_{mix} = \sum_{i=1,i\neq j}^{n} \Omega_{ij} c_i c_j \tag{2}$$

where $\Omega_{ij} = 4\Delta H_{mix}^{AB}$, ΔH_{mix}^{AB} is the mixing enthalpy of binary liquid AB alloys. The ΔH_{mix}^{AB} data for the atomic pairs A−B was taken from Ref. [26].

$$\Delta S_{mix} = -R\sum_{i=1}^{n} c_i \ln c_i \tag{3}$$

where R is the mole gas constant.

The enhancement of GFA can be explained by the empirical criteria suggested by TAKEUCHI and INOUE [27]. First, four components can be found in the alloy system. With increasing Cr content, the values of ΔH_{mix} and ΔS_{mix} are found to increase from −10.60 to −10.38 kJ/mol and from 6.34 to 7.29 kJ/(mol·K), respectively. According to "confusion principle" reported by GREER [28], the more elements involved, the lower the chance that the alloy can select viable crystal structures, and the greater the chance of glass formation. Second, the atomic sizes of Nb, Cr, Fe, and B are 0.14290, 0.12491, 0.12412, and 0.08200 nm, respectively [29]. The atomic size difference (δ) is larger than 15.02 for the $(Fe_{74}Nb_6B_{20})_{100-x}Cr_x$ (x=1, 3, 5) alloys, as shown in Table 2. The large atomic size difference among the main constituent elements is favorable for the increase of atomic packing density of the liquid structure. Additionally, there exist negative heats of mixing among the main constituent elements. The mixing enthalpies of the main constituent elements for Fe−Nb, Fe−B, and Fe−Cr pairs are −16, −11, and −1 kJ/mol, whereas those of additional elements for Nb−B, Nb−Cr, and B−Cr are −27, −7, and −16 kJ/mol [26], respectively. The negative mixing enthalpies of the atomic pairs between Fe−Nb, and Nb−B are larger than that of Fe−Cr, Fe−B, and Nb−Cr pairs. MATSUBARA et al [30] reported that the Fe−Nb−B glassy alloys consist of non-periodic network of the trigonal prisms in which the cubo-octahedra and the cubes formed by metal atoms are connected with metalloid atoms. The local atomic arrangement would reduce the diffusivity in the glassy state, and effectively suppress the crystallization process due to the difficulty

Table 2 Calculated thermodynamic parameters of $(Fe_{74}Nb_6B_{20})_{100-x}Cr_x$ (x=1, 3, 5) glassy alloys

Alloy	δ	ΔH_{mix}/ (kJ·mol^{-1})	ΔS_{mix}/ (kJ·mol^{-1}·K^{-1})
$(Fe_{74}Nb_6B_{20})_{99}Cr_1$	15.31	−10.60	6.34
$(Fe_{74}Nb_6B_{20})_{97}Cr_3$	15.14	−10.45	6.87
$(Fe_{74}Nb_6B_{20})_{95}Cr_5$	15.02	−10.38	7.29

of long-range rearrangement of the constituent elements. It is believed that the addition of Cr in Fe−Nb−B alloys results in more densely packed Fe−Nb−B skeletons, thus enhancing the GFA of the glassy alloys.

3.4 Soft magnetic property

Figure 3 shows magnetic hysteresis loops (*M*−*H*) of the $(Fe_{74}Nb_6B_{20})_{100−x}Cr_x$ (*x*=1, 3, 5) glassy alloys. It can be seen that the saturation magnetization (M_s) decreases from 161 A·m²/kg for the alloys with 1% Cr to 139 A·m²/kg for the alloys with 5%Cr. Cr is paramagnetic element, while Fe is of ferromagnetism. The outer electronic structures for Fe and Cr are $3d^64s^2$ and $3d^54s^1$, respectively, and Cr has fewer 3d electrons than Fe. The reason that Cr addition decreases the magnetic moment of Fe is related to the antiferromagnetic coupling to Fe moments [31]. OLIVIER et al [32] reported that Cr decreases the moment of Fe atom by 0.04 μ_B per mole fraction of Cr for $Fe_{80−x}Cr_xB_{20}$ (*x*<5) glassy ribbons. Consequently, the saturation magnetization drops remarkably with increasing Cr content.
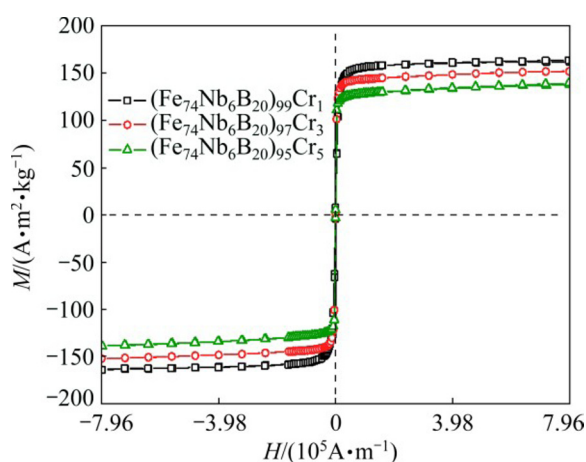
Fig. 3 Magnetization hysteresis curves (*M*−*H* loops) of $(Fe_{74}Nb_6B_{20})_{100−x}Cr_x$ (*x*=1, 3, 5) glassy alloys at room temperature

The H_c value depends mostly on surface and pinning effect of magnetic domain walls. Because of surface irregularities, the H_c value is proportional to the ratio of the surface roughness amplitude to the specimen thickness. This contribution to H_c should be high for ribbons, because the surface after casting is not very smooth and its width is several orders of magnitude larger than the thickness [11]. Additionally, the contribution of pinning effect to H_c is associated with the inclusions in the alloys. These inclusions mainly come from the raw materials, and they would act as pinning sites for magnetic domain walls inside amorphous alloys [14]. However, most inclusions can be removed after fluxing method, thus consequently resulting in a low coercivity.

Compared to the magnetic properties in other Fe-based amorphous alloys fabricated with high-purity raw materials (Table 3), the present Fe−Nb−B−Cr amorphous alloys exhibited excellent soft magnetic properties with high saturation magnetization and low coercivity. The saturation magnetization of the $(Fe_{74}Nb_6B_{20})_{100−x}Cr_x$ (*x*=1, 3, 5) glassy alloys are superior to that of $Fe_{65.5}Cr_4Mo_4Ga_4P_{12}C_5B_{5.5}$ (M_s=92.5 A·m²/kg) [33] and $Co_{50.4}Fe_{21.6}B_{19.2}Si_{4.8}Cr_4$ (M_s=106.1 A·m²/kg) [34]. Our newly developed $(Fe_{74}Nb_6B_{20})_{100−x}Cr_x$ (*x*=1, 3, 5) glassy alloys exhibit large GFA, excellent soft magnetic properties, and low manufacturing cost. These Fe-based glassy alloys are suitable for industrial production, and they are good candidate to extend the application field of amorphous materials, especially in the area of magnetic components for engineering application.

4 Conclusions

1) The $(Fe_{74}Nb_6B_{20})_{100−x}Cr_x$ glassy alloys were successfully fabricated using low-purity industrial raw materials. These newly developed Fe-based glassy alloys can extend the application fields of amorphous materials due to their low manufacturing cost, large GFA, and excellent magnetic properties.

2) The addition of Cr results in an improvement of GFA compared to that in the Cr-free Fe−Nb−B alloys while the values of T_g and T_x are not significantly changed with increasing Cr content. The $(Fe_{74}Nb_6B_{20})_{95}Cr_5$ alloy is found to exhibit the best GFA (ΔT_x=54 K).

3) The Cr-containing Fe-based glassy alloys exhibit excellent soft magnetic properties with high M_s of

Table 3 Comparison of soft magnetic properties between our newly developed $(Fe_{74}Nb_6B_{20})_{100−x}Cr_x$ (*x*=1, 3, 5) glassy alloys and other typical Fe-based metallic glasses

Sample	Diameter/mm	M_s/(emu·g⁻¹)	H_c/(A·m⁻¹)	Remark	Reference
$Fe_{65.5}Cr_4Mo_4Ga_4P_{12}C_5B_{5.5}$	Ribbon	92.5	1.7	High-purity elements	[33]
$Co_{50.4}Fe_{21.6}B_{19.2}Si_{4.8}Cr_4$	Ribbon	106.1	5.01	High-purity elements	[34]
$(Fe_{74}Nb_6B_{20})_{99}Cr_1$	Ribbon	161	52.54	Industrial raw materials	Present study
$(Fe_{74}Nb_6B_{20})_{97}Cr_3$	Ribbon	152	30.24	Industrial raw materials	Present study
$(Fe_{74}Nb_6B_{20})_{95}Cr_5$	Ribbon	139	58.90	Industrial raw materials	Present study

139−161 A·m^2/kg and low H_c of 30.24−58.90 A/m.

4) As Cr content increases, the GFA and thermal stability do not change significantly, while the magnetic properties decrease remarkably. For the alloys having excellent magnetic properties while maintaining high GFA and thermal stability, the optimal amount of Cr is less or equal to 3%.

References

[1] SHEN B L, INOUE A, CHANG C T. Superhigh strength and good soft-magnetic properties of (Fe, Co)−B−Si−Nb bulk glassy alloys with high glass-forming ability [J]. Applied Physics Letters, 2004, 85: 4911−4913.

[2] SHEN T D, SHWARZ R B. Bulk ferromagnetic glasses in the Fe−Ni−P−B system [J]. Acta Materialia, 2001, 49: 837−847.

[3] LU Z P, LIU C T, THOMPSON J R, PORTER W D. Structural amorphous steels [J]. Physical Review Letters, 2004, 92: 245503-(1−4).

[4] INOUE A. Stabilization of metallic supercooled liquid and bulk amorphous alloys [J]. Acta Materialia, 2000, 48: 279−306.

[5] LIN C Y, TIEN H Y, CHIN T S. Soft magnetic ternary iron-boron-based bulk metallic glasses [J]. Applied Physics Letters, 2005, 86: 162501−(1−3).

[6] YOSHIZAWA Y, OGUMA S, YAMAUCHI K. New Fe-based soft magnetic alloys composed of ultrafine grain structure [J]. Journal of Applied Physics, 1988, 64: 6044−6046.

[7] SUZUKI K, MAKINO A, INOUE A, MASUMOTO T. Low core losses of nanocrystalline Fe−M−B (M=Zr, Hf, or Nb) alloys [J]. Journal of Applied Physics, 1993, 74: 3316−3322.

[8] ZHANG Y, HONO K, INOUE A, MAKINO A, SAKURAI T. Nanocrystalline structural evolution in Fe$_{90}$Zr$_7$B$_3$ soft magnetic material [J]. Acta Materialia, 1996, 44: 1497−1510.

[9] MAKINO A, SUZUKI K, INOUE A, MASUMOTO T. Magnetic properties and core losses of nanocrystalline Fe−M−B (M=Zr, Hf or Nb) alloys [J]. Materials Science and Engineering A, 1994, 179−180: 127−131.

[10] MAKINO A, HATANAI T, INOUE A, MASUMOTO T. Nanocrystalline soft magnetic Fe−M−B (M = Zr, Hf, Nb) alloys and their applications [J]. Materials Science and Engineering A, 1997, 226−228: 594−602.

[11] STOICA M, HAJLAOUI K, LEMOULEC A, YAVARI A R. New ternary Fe-based bulk metallic glass with high boron content [J]. Philosophical Magazine Letters, 2006, 86: 267−275.

[12] YAO J H, WANG J Q, Li Y. Ductile Fe–Nb–B bulk metallic glass with ultrahigh strength [J]. Applied Physics Letters, 2008, 92: 251906−(1−3).

[13] YAO J H, YANG H, ZHANG J, WANG J Q, Li Y. The influence of Nb and Zr on glass-formation ability in the ternary Fe−Nb−B and Fe−Zr−B and quaternary Fe−(Nb,Zr)−B alloy systems [J]. Journal of Materials Research, 2008, 23: 392−401.

[14] LI H X, GAO J E, WANG S L, YI S, LU Z P. Formation, crystallization behavior, and soft magnetic properties of FeCSiBP bulk metallic glass fabricated using industrial raw materials [J]. Metallurgical and Materials Transactions A, 2012, 43: 2615−2619.

[15] GAN Z H, YI H Y, PU J, WANG J F, XIAO J Z. Preparation of bulk amorphous Fe−Ni−P−B−Ga alloys from industrial raw materials [J]. Scripta Materialia, 2003, 48: 1543−1547.

[16] XIE Chun-xiao, YANG Yuan-zheng, ZHONG Shou-yan, DENG Shi-chun. Effects of Co/Ni mole ratio on crystallization processes and magnetic properties of FeCoNiCrZr amorphous alloys [J]. The Chinese Journal of Nonferrous Metals, 2015, 25: 727−732.

[17] SONG D S, KIM J H, FLEURY E, KIM W T, KIM D H. Synthesis of ferromagnetic Fe-based bulk glassy alloys in the Fe−Nb−B−Y system [J]. Journal of Alloys and Compounds, 2005, 389: 159−164.

[18] ZHUANG Yan-xin, WANG Shen-ci, WANG Chang-jiu, WANG Nai-peng, HE Ji-cheng. Effect of Ti on microstructure, mechanical and corrosion properties of (Zr$_{0.55}$Al$_{0.1}$Ni$_{0.05}$Cu$_{0.3}$)$_{100−x}$Ti$_x$ bulk metallic glasses [J]. Transactions of Nonferrous Metals Society of China, 2016, 26: 138−143.

[19] HAN Jia-jia, WANG Cui-ping, KOU Sheng-zhong, LIU Xing-jun. Thermal stability, crystallization behavior, Vickers hardness and magnetic properties of Fe−Co−Ni−Cr−Mo−C−B−Y bulk metallic glasses [J]. Transactions of Nonferrous Metals Society of China, 2013, 23: 148−155.

[20] INOMATA K, HASEGAWA M, SHIMANUKI S. Magnetic properties of amorphous Fe−Cr−Si−B alloys [J]. IEEE Transactions on Magnetics, 1981, 17: 3076−3078.

[21] PANG S J, ZHANG T, ASAMI K, INOUE A. Formation of bulk glassy Fe$_{75−x−y}$Cr$_x$Mo$_y$C$_{15}$B$_{10}$ alloys and their corrosion behavior [J]. Journal of Materials Research, 2002, 17: 701−704.

[22] LONG Z L, SHAO Y, DENG X H, ZHANG Z C, JIANG Y, ZHANG P, SHEN B L, INOUE A. Cr effects on magnetic and corrosion properties of Fe–Co–Si–B–Nb–Cr bulk glassy alloys with high glass-forming ability [J]. Intermetallics, 2007, 15: 1453−1458.

[23] LU Z P, LI Y, NG S C. Reduced glass transition temperature and glass forming ability of bulk glass forming alloys [J]. Journal of Non-Crystalline Solids, 2000, 270: 103−114.

[24] LU Z P, LIU C T. A new glass-forming ability criterion for bulk metallic glasses [J]. Acta Materialia, 2002, 50: 3501−3512.

[25] ZHANG Y, ZHOU Y J, LIN J P, CHEN G L, LIAW P K. Solid-solution phase formation rules for multi−component alloys [J]. Advanced Engineering Materials, 2008, 10: 534−538.

[26] de BOER F R, BOOM R, MATTENS W C M, MIEDEMA A R, NIESSEN A K. Cohesion and structure, Vol. 1 [M]. Netherlands, North-Holland Physics Phublishing, 1988.

[27] TAKEUCHI A, INOUE A. Classification of bulk metallic glasses by atomic size difference, heat of mixing and period of constituent elements and its application to characterization of the main alloying element [J]. Materials Transactions, 2005, 46: 2817−2829.

[28] GREER A L. Confusion by design [J]. Nature, 1993, 336: 303−304.

[29] SENKOV O N, MIRACLEB D B. Effect of the atomic size distribution on glass forming ability of amorphous metallic alloys [J]. Materials Research Bulletin, 2001, 36: 2183−2198.

[30] MATSUBARA E, SATO S, IMAFUKU M, NAKAMURA T, KOSHIBA H, INOUE A, WASEDA Y. Structural study of Amorphous Fe$_{70}$M$_{10}$B$_{20}$ (M=Zr, Nb and Cr) alloys by X-ray diffraction [J]. Materials Science and Engineering A, 2001, 312: 136−144.

[31] MIZOGUCHI T. Magnetism in amorphous alloys [J]. AIP Conference Proceedings, 1976, 34: 286−291.

[32] OLIVIER M, STROM-OLSEN J O, ALTOUNIAN Z. Disorder and magnetic effects on the electron-transport properties of iron-chromium-boron metallic glasses [J]. Physical Review B, 1987, 35: 333−341.

[33] STOICA M, ROTH S, ECKERT J, SCHULTZ L, BARÓ M D. Bulk amorphous FeCrMoGaPCB: Preparation and magnetic properties [J]. Journal of Magnetism and Magnetic Materials, 2005, 290−291: 1480−1482.

[34] VELIGATL M, KATAKAM S, DAS S, DAHOTRE N, GOPALAN R, PRABHU D, BABU D A, CHOI-YIM H, MUKHERJEE S. Effect of iron on the enhancement of magnetic properties for cobalt-based soft magnetic metallic glasses [J]. Metallurgical and Materials Transactions A, 2015, 46: 1019−1023.

低纯度原料制备铁基非晶合金的
形成能力和磁学性能

朱 满，法 阳，坚增运，姚丽娟，靳长清，许军锋，南瑞华，常芳娥

西安工业大学 材料与化工学院，西安 710021

摘　要： 采用低纯度原料制备的$(Fe_{74}Nb_6B_{20})_{100−x}Cr_x$ (x=1, 3, 5)非晶合金具有高的玻璃形成能力(GFA)和良好的软磁性能。铬含量的增加并未显著影响合金的玻璃化转变温度和晶化起始温度，然而其使液相线温度显著增加。$(Fe_{74}Nb_6B_{20})_{100−x}Cr_x$ (x=1, 3, 5)合金的过冷液相区宽度(ΔT_x)，T_r和γ分别为50~54 K，0.526~0.538 和 0.367~0.371，比未添加铬的 Fe−Nb−B 合金的玻璃形成能力要强。$(Fe_{74}Nb_6B_{20})_{100−x}Cr_x$非晶合金软磁性能优异，其饱和磁感应强度为139~161 A·m²/g，矫顽力为30.24~58.90 A/m。制备得到的 Fe−Nb−B−Cr 非晶合金的玻璃形成能力高、软磁性能优异且成本低廉，是一款适用于工程应用的软磁材料。

关键词： 铁基非晶合金；铬；玻璃形成能力；磁学性能

(Edited by Yun-bin HE)